Available online at www.sciencedirect.com
SCIENCE DIRECT®
Journal of Molecular Catalysis A: Chemical 226 (2005) 231–234
JOURNAL OF MOLECULAR CATALYSIS A: CHEMICAL
www.elsevier.com/locate/molcata

Catalytic effect of laser ablated Ni nanoparticles in the oxidative addition reaction for a coupling reagent of benzylchloride and bromoacetonitrile

Sungil Kim[a], Bum Keun Yoo[a], Keunho Chun[a], Weekyung Kang[a], Jaebum Choo[b], Myoung-Seon Gong[c], Sang-Woo Joo[a,*]

[a] *Department of Chemistry, Soongsil University, CAMDRC (Computer Aided Molecular Design Research Center), Seoul 156-743, Republic of Korea*
[b] *Department of Applied Chemistry, Hanyang University, Ansan 425-791, Republic of Korea*
[c] *Department of Chemistry, Dankook University, Cheonan 330-714, Republic of Korea*

Received 20 June 2004; received in revised form 25 October 2004; accepted 26 October 2004

Abstract

We checked the catalytic activity of Ni nanoparticles prepared by pulsed-laser ablation. The transmission electron microscopy images showed that Ni metal particles would have an inhomogeneous size distribution of 5.7 (±3.8) nm. The UV absorbance spectrum exhibited metallic Ni characteristics. Ni nanoparticles appeared to exhibit the catalytic activity in the oxidative addition reaction without any activations for the preparation of 3-arylpropanenitrile from benzylchloride and bromoacetonitrile in glyme with a yield of ∼20%. We could not find this catalytic effect for the larger sizes of submicron, 3 μm, and 100 mesh Ni particles.

Keywords: Ni; Nanoparticles; Catalytic effect; Laser ablation

1. Introduction

Since physical properties of metals can vary depending on dimensions, the ability to prepare nanosized particles will open significant opportunities in chemistry and material science [1]. The catalytic activity of Au/TiO_2 for the CO oxidation reaction was found to depend on the size of Au clusters in diameter from 1 to 6 nm [2]. Magnetic properties of Ni nanowires prepared by electrodeposition were examined using vibrating sample magnetometer measurements [3]. Bifunctional AuNi nanorods were used for gene transfer since the carboxylate end group could bind to the Ni segment [4]. Ni complexes have been widely employed as catalysts in a variety of organic chemical reactions [5–10]. Although zerovalent Ni in the metallic state has not been known to usually undergo oxidative addition of organic halides under mild conditions, Rieke and coworkers reported that oxidative addition could occur from the metallic nickel prepared by the reduction of nickel halide with lithium [11–19].

Although chemical reduction of metal salts is one of the most frequently used methods for producing colloidal metals, laser ablation of a metal plate in solution is found to be an alternative method to prepare metal colloids [20]. One of the most important advantages of this approach is an absence of organic or ionic species in solution and its simplicity in sample preparation. Noble and transition metal nanoparticles have been prepared by such a laser ablation method [21,22]. Halide-modified laser ablated Ag colloids were found to reduce the cytochrome *c* [23]. The absence of organic stabilizers in addition to the small sizes of laser ablated transition metal particles are expected to show the enhanced catalytic effect in organic reactions. In this work, we report the catalytic activity of laser ablated Ni nanoparticles for a simple oxidative addition reaction of benzylchloride with bromoacetonitrile for the preparation of 3-arylpropanenitrile.

* Corresponding author. Tel.: +82 2 8200434; fax: +82 2 8200434.
E-mail address: sjoo@ssu.ac.kr (S.-W. Joo).

1381-1169/$ – see front matter © 2004 Elsevier B.V. All rights reserved.
doi:10.1016/j.molcata.2004.10.038

2. Experimental and methods

2.1. Preparation of Ni nanoparticles

The spherical nanoparticles were produced by irradiation of the Ni foil with or without adding $\sim 10^{-2}$ M of sodium dodecyl sulfate (SDS) as surfactants for stabilizing nanoparticles. Aqueous metal nanoparticle solutions could be produced by laser ablation using a second harmonic of Nd-YAG laser (Continuum Minilite II) at 532 nm with the delay time of ~200 μs. A 10 cm focal length lens was used to focus to irradiate the sample. Ni foil (99.99%) from Aldrich was initially placed and irradiated at the bottom of a plastic vessel filled with 7 ml of triply distilled water. The sample was obtained after the laser irradiation at ~30 mJ for 3 h on the metal foil. The laser power was checked by a power meter (Gentec TPM 300).

2.2. TEM and UV measurements

TEM images were obtained by JEOL JEM 3000F. The TEM sample was prepared by evaporating a drop of the sample solution on a copper mesh coated with carbon film. The size distribution was obtained by measuring the diameters of at least 150 particles. UV–vis absorbance spectrum of the Ni nanoparticle solution was taken using Shimadzu 3100 PC spectrophotometer.

2.3. Catalytic reaction

Benzylchloride, bromoacetonitrile, glyme, submicron, 3 μm, and 100 mesh Ni particles were purchased from Aldrich. A mixture of benzylchloride (124 mg, 82.67 μl, 0.982 mmol) and bromoacetonitrile (118 mg, 107.27 μl, 0.980 mmol) in glyme (0.5 ml) was added to the dissolved nickel nanoparticle solution in glyme (0.5 ml) by syringe [16]. This mixture was in reflux for 30 min. An additional heating was continued for 15 min, the mixture was cooled and poured into a separatory funnel containing 3% hydrochloric acid (10 ml), and was extracted with methylene chloride (15 ml). The combined extracts were washed with water (20 ml), dried with anhydrous sodium sulfate, and concentrated. The residual oil was purified by chromatography on silica gel eluting with methylene chloride. The product was checked by nuclear magnetic resonance spectroscopy using Bruker Avance 400 FT-NMR. ^{1}H NMR chemical shift δ: 2H, 2.50 ppm; 2H, 2.15 ppm; 5H, 7.31–7.39 ppm. Fig. 1 shows the scheme of organic reaction to check the catalytic activity.

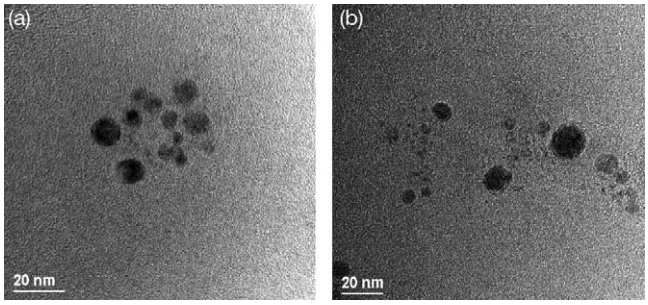

Fig. 2. High-resolution transmission electron microscopy image of Ni nanoparticles: (a) with or (b) without the addition of $\sim 10^{-2}$ M of SDS.

3. Results and discussion

Fig. 2 shows a high-resolution transmission electron microscopy (TEM) image taken for a selected Ni sample with and without the addition of $\sim 10^{-2}$ M SDS, respectively. Fig. 3a and b shows a size distribution of the Ni nanoparticles produced by laser ablation. The mean diameters of Ni nanoparticles were measured to be 5.7 (±3.8) nm. After the addition of $\sim 10^{-2}$ M SDS, the size and its distribution were found to be slightly smaller to be 5.2 (±2.3) nm with an elimination of larger particles with the diameter larger than 15 nm as shown in Fig. 2b. Although more controlled experiments at different laser conditions and surfactant concentrations should be performed, SDS appeared not to change greatly the size and size distribution of Ni particles, differently from the case of Pt particles [21]. Dissimilar physical properties of Ni would result in the deviating growth mechanism during laser ablation.

Several growth mechanisms can be suggested for the Ni nanoparticles. Since the irradiated spot of a metal plate surface will locally reach a very high temperature instantaneously after by laser ablation, a photo-annealing process would lead a growth of nanoparticles. It has been reported that the plasma-confined bubbles should be instantaneously generated at high temperature and pressure for the initial stage of nanoparticle formation by a laser impact on the metal plate in the liquid phase [24]. The nucleation and growth process of Ni nanoparticles in the liquid phase could be explained by the dynamic formation mechanism [21]. Contiguously after the laser irradiation on a nickel metal plate immersed in the solution, the atoms in a plume formed over the laser spot would conglomerate rapidly into small particles as the atoms interfuse mutually. Until the free atoms in the vicinity are completely used, a further nucleation should continue to make larger nickel particles in the solution. Such

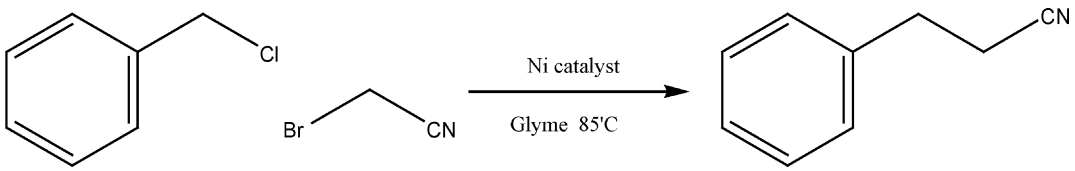

Fig. 1. Scheme of oxidative addition to check the catalytic activity of Ni nanoparticles.

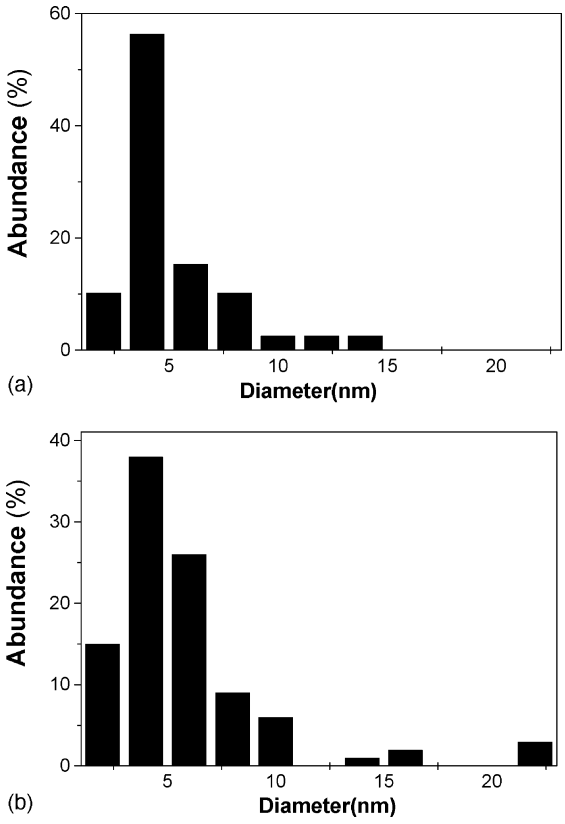

Fig. 3. Size distribution of Ni nanoparticles: (a) with or (b) without adding SDS.

nanoparticles would grow slowly by attracting free Ni atoms and diffuse into the solution resulting in a colloidal dispersion. For Ni metal colloids prepared by laser ablation, the shape of nanoparticles is nearly isotropic.

Our UV spectrum indicated metallic nickel characteristics in the solution [25] as shown in Fig. 4. UV–vis absorbance spectra showed the feature at ∼205 nm due to the Ni particle solution. The weak and broad band at ∼350 nm for nickel nanoparticles in the previous report [26] was not conspicuous in our UV spectrum. However, for the oxide of nickel particles, the electronic bands should shift to a longer wavelength region [27]. Such oxide peaks were not clearly identified either. Although an XPS study [26] should be quite informative to confirm the oxidation state of our Ni particles it was difficult to prepare enough Ni nanoparticle samples for an XPS measurement. A further characterization of the sample by a more efficient production of Ni nanoparticles by optimizing laser ablation condition is in progress to reach a precise conclusion on the oxidation state.

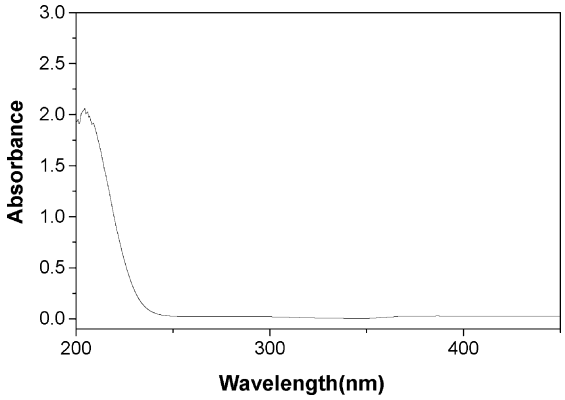

Fig. 4. UV–vis absorption spectrum of laser ablated Ni nanoparticles in solution.

Ni nanoparticles presumably with its zero valence state should show the catalytic activity for the preparation of 3-arylpropanenitrile from benzylchloride and bromoacetonitrile in glyme with a yield of ∼20% under the mild condition without any activation. We could not find this catalytic effect for the commercial submicron, 3 μm, and 100 mesh Ni particles, however. Our laser ablated Ni particles with the diameter of ∼5 nm are supposed to have higher catalytic activity due to their smaller size and larger surface area. The absence of organic stabilizers in addition to the small sizes of laser ablated transition metal particles are expected to show the enhanced catalytic effect in organic reactions.

It is admitted that we failed to increase the yield of the catalytic reactions of Ni nanoparticles presumably due to a facile oxide formation on the surface of Ni particles, however. Only the laser ablated Ni particles without adding stabilizers showed the catalytic activities. Although the presented oxidative addition reaction has been reported to occur for the zero valence state, it is possible that the oxidation reaction could occur on the nickel nanoparticle surfaces in the solution phase. Such a low yield (∼20%) even for nanosized nickel particles in the diameter of ∼5 nm suggests that the surface of nickel particles could be oxidized at least partially. Inferring from the previous report [26] for preparation of nickel nanoparticles, it is likely that the nickel and nickel oxide nanoparticle would coexist in the solution. A more detailed study is in progress to better understand the catalytic stabilities of Ni nanoparticles.

To check the catalytic activity reaction for the laser ablated nickel particles, benzylchloride and bromoacetonitrile are chosen for the present case mainly due to its simplicity in the oxidative addition. In the previous report [16], its yield for 3-arylpropanenitrile was 57 and 21% with and without refluxing in the glyme, respectively. These yields were not greatly high for the other compounds used in the oxidative addition reaction. We plan to check and compare the other compounds in the future by optimizing each catalytic condition.

Colloidal nanoparticles in solution are assumed to be promising candidates for catalytic reactions because of their uniform dispersion and reusability. Recently, there have been quite a few reports [28,29] on the catalytic activities for the supported metal nanoparticle catalysts. It will be interesting to check the catalytic activity for supported nickel nanoparticles on different substrates. Our future research should lie in the development for facile and efficient catalysts based on nanoparticles under various fabrication conditions.

It is admitted that free nickel atoms dispersed in the solution would lead the catalytic reaction also in a homogeneous way under the same phase condition. In our present study, the catalytic reaction was assumed to occur mainly heterogeneously or semi-heterogeneously on the surface of the nickel nanoparticles. A fairly well dispersed catalytic nickel particles in the solution however suggests a heterogeneous reaction.

Due to its small amount prepared by laser ablation, it was difficult to check the oxidation state of our Ni nanoparticles from other X-ray spectroscopic tools. It seems that Ni nanoparticles appeared to be easily oxidized at ambient conditions during the sample preparation. Our previous study using X-ray diffraction shows that gold nanoparticles have a polycrystalline surface with a prevalent (1 1 1) plane [30]. A more detailed analysis of crystal planes and compositions for Ni nanoparticles is in progress. An irradiation wavelength close to an intense surface plasmon resonance of Ni may affect a shape or a size distribution of the sample. We plan to study the shape and size distribution as a function of the irradiation wavelength and laser power of Nd-YAG laser.

4. Summary and conclusions

Ni nanoparticles prepared by pulsed-laser ablation was characterized by UV absorption spectroscopy and high-resolution transmission electron microscopy. The laser ablated Ni nanoparticles in solution with the zero-valence state presumably mixed with oxide forms exhibited a catalytic effect for the preparation of 3-arylpropanenitrile from benzylchloride and bromoacetonitrile under the mild condition without any activation whereas the Ni particles larger than submicrometer size have not shown this activity.

Acknowledgements

S-WJ would like to thank Prof. Kwan Kim for introduction to laser-ablated nanoparticle research and Dr. Sung Jin Bae for valuable comments on catalytic reactions. This work was supported by the ABRL program of Korean Science and Engineering Foundation (KOSEF Grant No. R-14-2002-004-01002-0). This work was supported by grant No. R01-2002-000-00378-0 from the Basic Research Program of the Korea Science and Engineering Foundation. We thank the Ministry of Science and Technology, Korea (No. M1-0213-03-0005), for financial support.

References

[1] G. Schmid (Ed.), Clusters and Colloids, VCH, Weinheim, 1994.
[2] M. Valden, X. Lai, D.W. Goodman, Science 281 (1998) 1647.
[3] L. Sun, P.C. Searson, C.L. Chen, Appl. Phys. Lett. 79 (2001) 4429.
[4] A.K. Salem, P.C. Searson, K.W. Leong, Nat. Struct. Mater. 2 (2003) 668.
[5] H. Zhang, W. Huang, L. Pu, J. Org. Chem. 66 (2001) 481.
[6] C. Cai, V.A. Soloshonok, V.J. Hruby, J. Org. Chem. 66 (2001) 1339.
[7] S. Iwasa, H. Maeda, K. Nishiyama, S. Tsushima, Y. Tsukamoto, H. Nishiyama, Tetrahedron 58 (2002) 8281.
[8] V. Humblot, S. Haq, C. Muryn, W.A. Hofer, R. Raval, J. Am. Chem. Soc. 124 (2002) 503.
[9] H. Brunner, H.B. Kagan, G. Kreutzer, Tetrahedron 14 (2003) 2177.
[10] H. Ueki, T.K. Ellis, C.H. Martin, T.U. Boettiger, S.B. Bolene, V.A. Soloshonok, J. Org. Chem. 68 (2003) 7104.
[11] A.V. Kavaliunas, R.D. Rieke, J. Am. Chem. Soc. 102 (1980) 5944.
[12] S. Inaba, H. Matsumoto, R.D. Rieke, Tetrahedron Lett. 23 (1982) 4215.
[13] H. Matsumoto, S. Inaba, R.D. Rieke, J. Org. Chem. 48 (1983) 840.
[14] S. Inaba, R.D. Rieke, Tetrahedron Lett. 24 (1983) 2451.
[15] S. Inaba, H. Matsumoto, R.D. Rieke, J. Org. Chem. 49 (1984) 2093.
[16] S. Inaba, R.D. Rieke, Synthesis (1984) 842.
[17] S. Inaba, R.D. Rieke, J. Org. Chem. 50 (1985) 1373.
[18] S. Inaba, R.D. Rieke, Tetrahedron Lett. 26 (1985) 155.
[19] S. Inaba, R.M. Wehmeyer, M.W. Forkner, R.D. Rieke, J. Org. Chem. 53 (1988) 339.
[20] M. Procházka, P. Mojzes, J. Stepánek, B. Vicková, P.-Y. Turpin, Anal. Chem. 69 (1997) 5103.
[21] F. Mafuné, J.-Y. Kohno, Y. Takeda, T. Kondow, J. Phys. Chem. B 107 (2003) 4218.
[22] M.F. Becker, J.R. Brock, H. Cai, D.E. Henneke, J.W. Keto, J. Lee, W.T. Nichols, H.D. Glicksman, NanoStruct. Mater. 10 (1998) 853.
[23] M. Sibbald, G. Chumanov, T.M. Cotton, J. Phys. Chem. 100 (1996) 4672.
[24] T. Tsuji, Y. Tsuboi, N. Kitamura, M. Tsuji, Appl. Surf. Sci. 229 (2004) 365.
[25] J.A. Creighton, D.G. Eaton, J. Chem. Soc., Faraday Trans. 87 (1991) 3881.
[26] X. Xiang, X.T. Zu, S. Zhu, L.M. Wang, Appl. Phys. Lett. 84 (2004) 52.
[27] G. Boschloo, A. Hagfeldt, J. Phys. Chem. B 105 (2001) 3039.
[28] A.M. Molenbroek, J.K. Nørskov, B.S. Clausen, J. Phys. Chem. B 105 (2001) 5450.
[29] H. Yang, W. Vogel, C. Lamy, N. Alonso-Vante, J. Phys. Chem. B 108 (2004) 11024.
[30] S.J. Bae, C.-R. Lee, I.S. Choi, C.-S. Hwang, M.-S. Gong, K. Kim, S.-W. Joo, J. Phys. Chem. B 106 (2002) 7076.